Physical Characterization of Electrochemically and Chemically Synthesized Polypyrroles

J. Joo*

Department of Physics and Center for Electro & Photo Responsive Molecules, Korea University, Seoul 136-701, Korea

J. K. Lee and S. Y. Lee

Department of Physics, Korea University, Seoul 136-701, Korea

K. S. Jang and E. J. Oh

Department of Chemistry, Myongji University, Yong-In 449-728, Korea

A. J. Epstein

Department of Physics and Department of Chemistry, The Ohio State University, Columbus, Ohio 43210-1106

Received August 19, 1999; Revised Manuscript Received April 12, 2000

ABSTRACT: The results of temperature-dependent dc conductivity, EPR magnetic susceptibility, and X-ray photoelectron spectroscopy (XPS) experiments are compared for electrochemically and chemically synthesized polypyrrole (PPy) samples. For chemically synthesized PPy samples soluble in organic solvent with large size dopants such as dodecylbenzenesulfonic acid (DBSA) or naphthalenesulfonic acid (NSA), dc conductivity (σ_{dc}) is ≤0.1 S/cm at room temperature, and its temperature dependence [$\sigma_{dc}(T)$] shows strong localization behavior, while $\sigma_{dc}(T)$ of the electrochemically synthesized PPy samples doped with hexafluorophosphate (PF_6) is in the critical or the metallic regime. The density of states of chemically prepared PPy−DBSA samples is less than one-fourth that of electrochemically synthesized PPy−PF_6 samples. The *g* values and temperature dependence of the line width obtained from EPR experiments show that the paramagnetic signals in both electrochemically and chemically synthesized PPy samples are mainly due to the polarons in π-conjugated polymer chains. We observe the existence of one dopant per three pyrrole rings in PPy−DBSA and PPy−PF_6 samples. From the XPS experiments, one-fifth of the pyrrole rings of chemically prepared PPy−DBSA are incorporated into interchain links or side chains, while for electrochemically prepared PPy−PF_6, one-third of the pyrrole units are in side chains or cross-links. We analyze that the side chains or cross-links of chemically synthesized PPy samples are relatively reduced, and subsequently the interchain interaction weakens. For chemically synthesized PPy samples, the synthesis method using large size dopants is one of the important roles for the reduction of side chains or cross-links and for the increase of solubility. The weakness of the interchain interaction and the reduction of side chains or interchain links for PPy systems play an important role for charge transport.

Introduction

The effects of doping in conducting polymers such as polyacetylene, polyaniline (PAN), or polypyrrole (PPy) show a transition similar to that of conventional semiconductors.[1] However, there are fundamental distinctions between these two systems. The morphological unit of conducting polymers is a quasi one-dimensional (1D) conjugated polymer chain, with covalent bonding along the chains and weak bonding between chains, whereas conventional semiconductors have three-dimensional (3D) structures. The anisotropic conductivity, dielectric constant, and thermoelectric power have been reported for conducting polymers.[1,2] The dopant ions in conducting polymers are positioned interstitially between polymer chains, while the dopant ions in conventional semiconductors generally are substituted directly into the host lattice. Interesting physical phenomena related to the dopants have been observed for conducting polymers. For example, the interchain interaction (or interchain hopping) between polymer chains has been emphasized to explain the variation of conductivity in both experiment and theory,[3,4] and the interactions between polymer backbones and dopants, or dopants and solvents, have been studied by use of dopants of various sizes in differing organic solvents.[1,5,6]

The dc conductivity (σ_{dc}) of PPy is changed through the doping process from insulating ($\sigma_{dc} \leq 10^{-7}$ S/cm) to metallic ($\sigma_{dc} \geq 10^2$ S/cm). To account for the variation of σ_{dc} due to doping, the presence of a polaron lattice or partially filled energy band has been proposed for the highly doped polymers.[1] The structure and the charge transport of doped PPy have been studied for electrochemically synthesized samples only. Pfluger and coworkers reported the existence of ∼33% interchain links (connected to the nearest polymer backbones) or side chains (connected to one polymer backbone) through the 2,3 positions in the pyrrole ring on the basis of an X-ray photoelectron spectroscopy (XPS) study of electrochemically synthesized PPy samples, while most of the pyrrole units are linked at the 2,5 positions to form straight chain as shown in Figure 1.[7,8] The synthesis method using relatively large dopants such as dodecylbenzenesulfonic acid (DBSA) or naphthalenesulfonic acid (NSA)

* To whom correspondence should be addressed. Email: jjoo@kuccnx.korea.ac.kr. Fax: +82-2-927-3292.

10.1021/ma991418o CCC: $19.00
Published on Web 06/20/2000

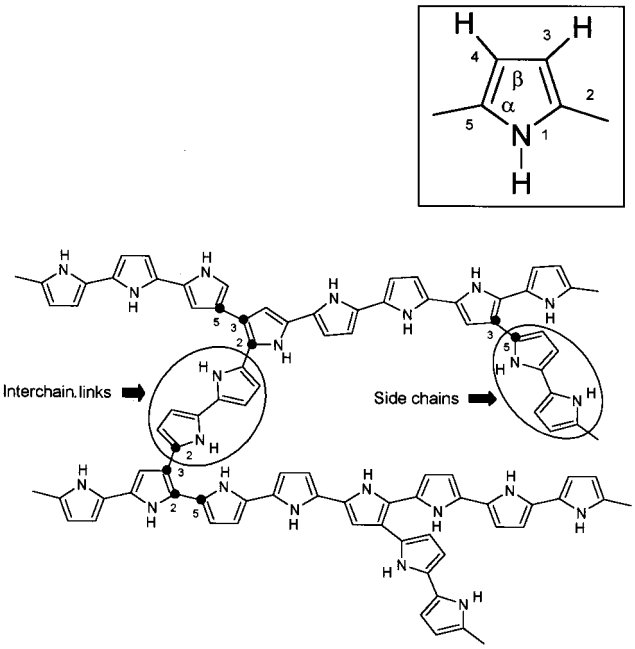

Figure 1. Schematic chemical structure of interchain links or side chains through 2,3 coupling modes of polypyrrole. Inset: pyrrole monomer with the conventional labeling of atom positions shown.

reduces the interchain interaction of polymer chains, resulting in the increase of the solubility in various organic solvents.[9,10]

In this paper, the results of the temperature-dependent dc conductivity, the density of states, the EPR line width (ΔH_{p-p}) and g values, and XPS experiments are compared for electrochemically synthesized PPy doped with hexafluorophosphate (PF_6), PPy−PF_6, and chemically synthesized PPy soluble in *m*-cresol solvent with DBSA or NSA dopants, PPy−DBSA (*m*-cresol) or PPy−NSA (*m*-cresol), respectively. We observe that the percent of interchain links or side chains of PPy−DBSA (*m*-cresol) samples is reduced by ∼10% compared to that of electrochemically synthesized PPy−PF_6 samples. This induces the reduction of the number of doping centers, and the relatively large dopants used results in weak interchain interaction, low σ_{dc}, and strong charge localization, reflecting the insulating state of soluble PPy systems. However, PPy−PF_6 samples with a relatively high concentration of interchain links or side chains show critical or metallic behavior. From the temperature dependence of the magnetic susceptibility, we obtain that the density of states of electrochemically synthesized PPy samples is higher than that of chemically synthesized PPy samples.

Experimental Section

The synthetic method of chemically synthesized PPy−DBSA and PPy−NSA samples soluble in *m*-cresol solvent was reported earlier.[10] For the synthesis of electrochemical PPy−PF_6 samples, 99% pure pyrrole was used.[11] Tetraethylammonium hexafluorophosphate ($TEAPF_6$) was used for an electrolyte. The anodic oxidation of pyrrole was carried out in an electrolyte bath including $TEAPF_6$ (0.1 mol), pyrrole (0.2 mol), and acetronitrile (AN) solvent. The materials were synthesized at 1.21 V for 5 h by using an EG & G PAR model 270A potentiostat/galvanostat. The samples were washed by using the mixture of water and AN solvent, and dried in a vacuum oven for 72 h. Both chemically and electrochemically prepared samples studied here were in the form of free-standing films of ∼60 and ∼200 μm thickness, respectively. The mass density

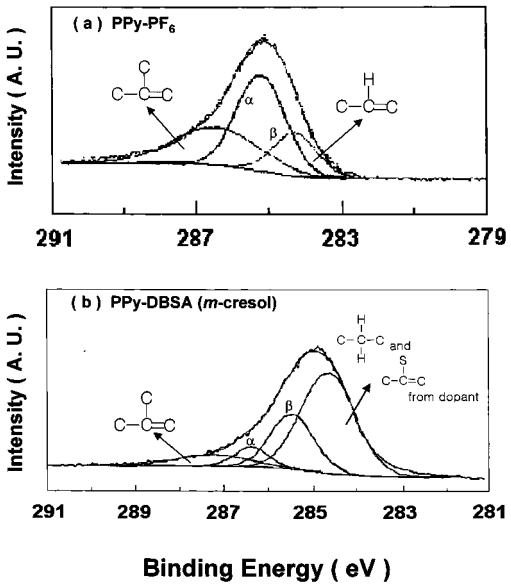

Figure 2. Carbon 1s (C1s) XPS core level spectrum of (a) PPy−PF_6 and (b) PPy−DBSA (*m*-cresol) samples. The top line through the data represents the best fit obtained from the superposition of the Gaussian peaks of the lower lines.

of PPy−DBSA (*m*-cresol) and PPy−PF_6 samples is ∼1.2 and ∼0.99 g/cm^3, respectively. The mass density of chemically synthesized PPy−DBSA (*m*-cresol) samples is slightly higher than that of electrochemically synthesized PPy−PF_6 samples because of the higher mass of the DBSA dopant. It is noted that, when PF_6 dopants were used, the solubility of PPy powder in organic solvents was reduced, resulting in difficulty in making free-standing films.

The EPR spectra for measuring magnetic susceptibility (χ), the g values, and ΔH_{p-p} were obtained by using a Bruker ESP 300 (X-band) spectrometer.[10] The measured temperature range of the EPR experiments was from 300 to 100 K. The magnetic susceptibility of the system was estimated from the EPR integrated intensities calibrated against a Li−LiF crystal standard. The XPS data were measured using a VG ESCALAB MkII spectrometer (Mg Kα X-ray source, 1253.6 eV photons). All binding energies were referenced to the C(1s) neutral carbon peak set at 284.6 eV to compensate for surface charging effects. The area ratios corrected by the sensitivity factor were used for the quantitative analysis of the XPS data. A four-probe technique was used for measuring dc conductivity to eliminate contact resistance.[6] Four thin gold wires (0.05 mm thick and 99% pure gold) were attached in parallel on the sample surface by conducting graphite paint (Acheson Electrodag 502) for better electrical contact. The measured temperature range for σ_{dc} was from 300 to 10 K using a Janis closed-cycle refrigerator system (CCS-100).

Results and Discussion

Figure 2 presents the carbon 1s (C1s) XPS core level spectrum of polypyrrole systems at room temperature (RT). For electrochemically synthesized PPy−PF_6 samples, a standard line shape analysis with Gaussian fitting shows that the C1s main peak is decomposed into three lines as shown in Figure 2a. The line due to the pyrrole β carbons is centered at 284.33 eV, while that of the α carbons in the pyrrole ring is positioned at 285.27 eV. There is ∼0.94 eV energy splitting between the two lines, which agrees with the observed energy separation in the pyrrole monomer.[7,12] The C1s spectrum is not symmetric on the higher binding energy side of the peak. This asymmetry was assigned to "disorder effects" such as interchain links, side chains, or chain terminations.[7,8] When disorder effects exist, the hydro-

Table 1. Measured Area Ratio (atom %) of the Composition of PPy−PF_6 and PPy−DBSA (*m*-Cresol) Samples Obtained from the Wide Scan of XPS Experiments

	area ratio (atom %)	
composition	PPy−PF_6	PPy−DBSA (*m*-cresol)
C	58.8	71.2
N	11.2	6.7
O	20.0	19.8
P	3.8	N/A
F	6.2	N/A
S	N/A	2.3
relative ratio	[P]/[N] = 33.9%	[S]/[N] = 34.3%

gen atom binding with the β carbon of the pyrrole rings is mainly changed to the carbon atom, which induces the higher binding energy and larger line width compared to α and β carbons, as shown in Figure 2. The measured area ratio of the disorder effects to the sum of three peaks assigned to α and β sites and the disorder effects is 0.33, in agreement with the report of Pfluger and Street.[7] For the chemically synthesized PPy−DBSA (*m*-cresol), the C1s main peak is decomposed into four lines including the covalently bonded carbon in the DBSA dopant, which corresponds to the lowest binding energy centered at 284.66 eV, as shown in Figure 2b. This lowest binding energy peak mainly originates from the carbons in the dodecyl group and the ones in the benzene ring binding with the sulfur of the DBSA dopant. The binding energy of the ortho carbons and meta carbons of the benzene ring of the DBSA dopant is the same as that of the pyrrole β carbons. The line due to the pyrrole β carbons is centered at 285.47 eV, while that of the α carbons is positioned at 286.37 eV. The overall shift of the peaks of the α and β carbons and the disorder effects as compared to those of electrochemically prepared PPy samples is due to the effect of charging. But the ∼0.90 eV energy splitting between the α and β carbons is maintained here. The measured area ratio of the disorder effects assumed due to interchain links, side chains, or chain terminations is ∼22%, which is a one-third reduction as compared to that of PPy−PF_6 samples. The results support reduction of the 2,3 coupling modes and relatively weak bonding between the chains. Table 1 shows the measured area ratio (atom %) of the composition of both doped PPy samples obtained from the wide scan of XPS experiments. From the analysis of the measured area ratio of the phosphorus ([P]) (or sulfur ([S])) to nitrogen ([N]), the [P]/[N] is ∼33.9% for PPy−PF_6 samples, and the [S]/[N] is ∼34.3% for PPy−DBSA (*m*-cresol) samples. The result implies the existence of one dopant per three pyrrole rings in PPy−DBSA(*m*-cresol) and PPy−PF_6 samples. The error in the XPS curve fitting is ∼5%.

Figure 3 compares the nitrogen 1s (N1s) XPS core level spectra of PPy materials at RT. The N1s signal originates from the nitrogen of the pyrrole rings of the polymer backbone because of lack of nitrogen in the dopants used. The spectrum of the N1s of PPy−PF_6 samples is asymmetric, while that of soluble PPy−DBSA (*m*-cresol) is relatively symmetric. The two higher binding energy peaks are separated from the neutral nitrogen peak by ∼1.30 and ∼2.68 eV as shown in Figure 3a,b. The shoulder on the higher energy side is assigned to an electrostatic effect of the nearest counterion.[7] This electrostatic effect is relatively weak for soluble PPy−DBSA (*m*-cresol) materials. Comparing the size of the dopant ions, the electric field due to the large

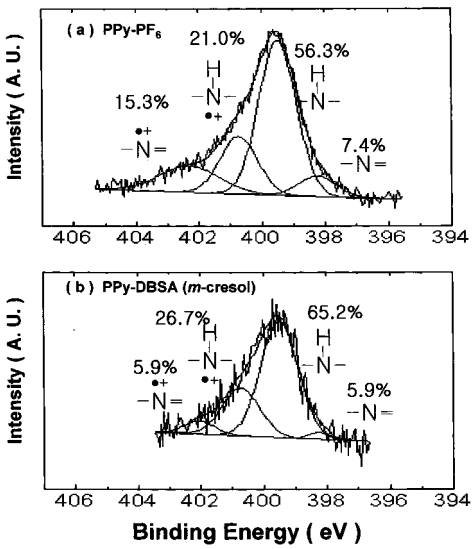

Figure 3. Nitrogen 1s (N1s) XPS core level spectrum of (a) PPy−PF_6 and (b) PPy−DBSA (*m*-cresol) samples. The top line through the data represents the best fit obtained from the superposition of the Gaussian peaks of the lower lines.

size $DBSA^-$ counterion is relatively weak. This implies that the interchain interaction of soluble PPy systems with the DBSA dopant is weak compared to that of the electrochemically synthesized PPy doped with PF_6. From the analysis of the N1s peak, we determine that the reduced segments of the pyrrole rings, which correspond to the peak positioned at 399.50 eV in Figure 3, exist at ∼65% and ∼56% for PPy−DBSA (*m*-cresol) and PPy−PF_6 samples, respectively. The two decomposed peaks centered at 400.80 and 402.30 eV in Figure 3 can be assigned to the protonation on the nitrogen site.[13] As shown in Figure 3a,b, the protonation level on the nitrogen site is ∼36% and ∼33% for electrochemically synthesized PPy−PF_6 and chemically synthesized PPy−DBSA (*m*-cresol) samples, respectively. It is noted that the polarons (π-electron radicals) are also formed on the carbon site of the quinoid (nonaromatic) rings of electrochemically and chemically synthesized PPy materials.

The density of states, $N(E_F)$, was obtained from the measurement of susceptibility (χ) through EPR experiments. Figure 4 presents χT as a function of temperature (T). The total magnetic susceptibility is described as

$$\chi = \chi^{\text{Pauli}} + \chi^{\text{Curie}} \tag{1}$$

where χ^{Pauli} is the Pauli susceptibility (independent of temperature) and χ^{Curie} is the Curie susceptibility (proportional to $1/T$). From the relation $\chi T = \chi^{\text{Pauli}} T + C$, where C is the Curie constant, the slope of χT vs T provides χ^{Pauli}.[14] Using the relation $\chi^{\text{Pauli}} = 2\mu_B^2 N(E_F)$, where μ_B is the Bohr magneton and $N(E_F)$ is the density of states at the Fermi level for one sign of spins, $N(E_F)$ is estimated as ∼0.333, ∼0.107, and ∼0.072 state/(eV ring) for PPy−PF_6, PPy−NSA (*m*-cresol), and PPy−DBSA (*m*-cresol) materials, respectively. The results imply that the electrochemically synthesized PPy−PF_6 with its relatively small dopant is in a highly conducting state compared to that of the doped soluble PPy materials, because the number of doping centers per unit volume might increase due to the increase of interchain links or side chains.

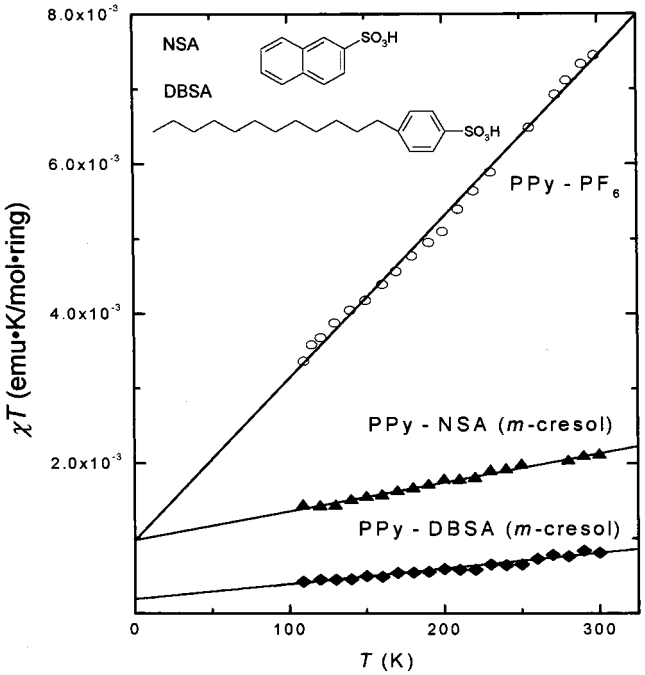

Figure 4. χT vs T for PPy−PF_6 (circles), PPy−NSA (*m*-cresol) (solid triangles), and PPy−DBSA (solid tilted squares). Inset: chemical structure of NSA and DBSA dopants.

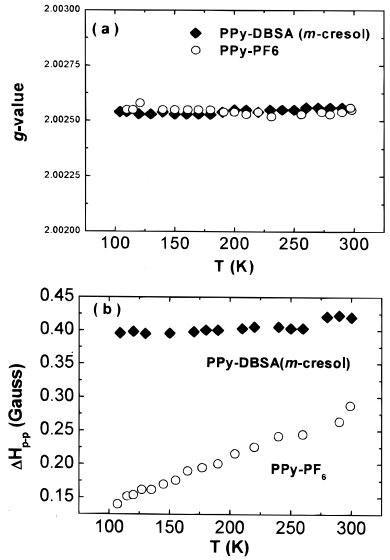

Figure 5. Comparison of temperature dependence of (a) the g values and (b) the EPR line width (ΔH_{p-p}) for PPy−PF_6 (circles) and PPy−DBSA (*m*-cresol) (solid tilted squares) samples.

Figure 5 shows the temperature dependence of the g values and ΔH_{p-p} for PPy−PF_6 and PPy−DBSA (*m*-cresol) materials. The g values for electrochemically and chemically prepared PPy samples are ∼2.0025, and independent of temperature from 300 to 100 K as shown in Figure 5a. It is noted that the principle g value in π-electron radicals from the free-spin value is 2.0023. The deviation of the g values is associated with spin−orbit interaction between the ground-state and excited-state radicals.[15] The variation of the ΔH_{p-p} of both doped PPy samples from 300 to 100 K is less than 0.25 G as shown in Figure 5b. These results indicate that the paramagnetic signals in both electrochemically and chemically synthesized PPy samples originate from the delocalized π-radicals in π-conjugated systems, i.e., polarons.[15−17]

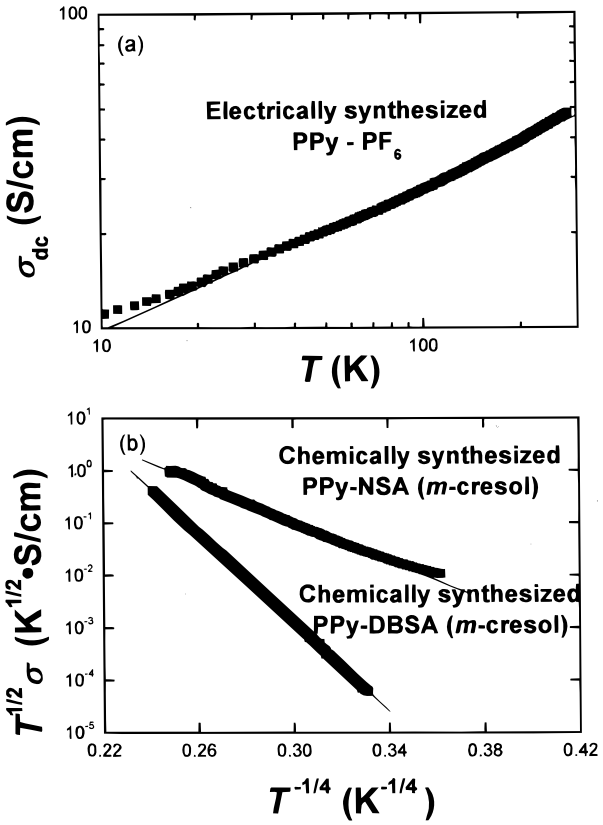

Figure 6. Comparison of the dc conductivity of (a) PPy−PF_6 and (b) PPy−NSA (*m*-cresol) and PPy−DBSA (*m*-cresol) samples, as a function of temperature.

Figure 6 compares the temperature dependence of the dc conductivity [$\sigma_{dc}(T)$] for electrochemically synthesized PPy−PF_6 and chemically synthesized PPy−DBSA and PPy−NSA samples soluble in *m*-cresol solvent. The σ_{dc}(RT) of the PPy−PF_6 samples studied here is ∼50 S/cm. A power law provides the best fitting for σ_{dc}(T) of PPy−PF_6 samples:

$$\sigma_{dc}(T) \propto T^{\beta} \tag{2}$$

where $1/3 < \beta < 1$. As shown in Figure 6a, β is ∼0.5, which implies that the materials are in the critical regime in the insulator−metal transition, or close to the metallic regime.[18,19] For soluble PPy samples, σ_{dc}(RT) is $\leq 10^{-1}$ S/cm, much lower than that of the electrochemically synthesized PPy−PF_6. The three-dimensional (3D) variable range hopping (VRH) model provides the best fitting for $\sigma_{dc}(T)$ of the chemically synthesized PPy samples:

$$\sigma_{dc} = \sigma_0 T^{-1/2} \exp[-(T_0/T)^{1/4}] \tag{3}$$

Here $T_0 = 16/[k_B N(E_F) L^3]$, $N(E_F)$ is the density of states at the Fermi level, and L is the localization length.[20] The slope T_0 [∼9.1×10^7 K for PPy−DBSA (*m*-cresol) and ∼3.0×10^6 K for PPy−NSA (*m*-cresol)] can be interpreted as the effective energy separation between localized states. By using the results of $N(E_F)$ obtained from EPR experiments, the localization length L is estimated as ∼4 and ∼2 Å for PPy−NSA (*m*-cresol) and PPy−DBSA (*m*-cresol) samples, respectively, indicating that the charge is strongly localized in soluble PPy systems. The interchain links or side chains of PPy systems provide extra doping centers in addition to the

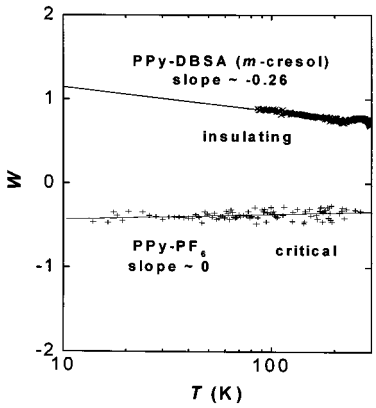

Figure 7. Temperature dependence of the reduced activation energy W of PPy−PF_6 and PPy−DBSA (*m*-cresol) samples.

polymer backbones. These might contribute to the 3D VRH of the poorly conducting PPy materials. The charge transport properties of soluble PPy materials also vary with the solvents used due to the screen effects of the polar solvents or the interactions among the solvent, the dopants, and the polymer backbones.[10] The effects of the dopant size of the electrochemically synthesized PPy samples on $\sigma_{dc}(T)$ were reported previously by Sato et al.[21] They observed that the system becomes more highly conducting as the size of the dopants decreases.

Figure 7 compares the $\sigma_{dc}(T)$ of the PPy materials studied here using the reduced activation energy defined as[18]

$$W(T) = \log \frac{\mathrm{d} \ln \sigma_{dc}(T)}{\mathrm{d} \ln T} \qquad (4)$$

From the slope of the $W(T)$ plot, one can determine the insulating, critical, or metallic state of the materials. The slope of soluble PPy samples is negative, i.e., W increases as T decreases, which indicates that the systems are in the insulating regime. However, the slope of the $W(T)$ plot of PPy−PF_6 samples is estimated to be 0 or even positive, indicating that the systems are in the critical or the metallic regime.

On the basis of the results studied here, the PPy systems can be considered as quasi network systems through the 2,3 coupling modes as shown in Figure 1. Though the 2,3 coupling modes might increase the mechanical strength, and provide the extra doping centers, they induce the reduction of the solubility of PPy in organic solvents and variation of the conjugation length. Experimentally, the effects of interchain links or side chains on physical properties have not been reported for doped polyacetylene and PAN systems, which have been considered as quasi one-dimensional structures.[1,2] Prigodin et al. theoretically studied a random network model of metallic wires[22] and also percolation in a fractal network,[23] in which the insulator−metal transition of conducting polymers can be determined by the concentration of the junctions such as interchain links or side chains. The charges of soluble PPy samples are strongly localized, and the system is in the insulating regime. Though the larger electrostatic effect of PF_6 encourages localization, it also induces the strong interchain interaction.

Conclusions

Charge transport and structural properties of electrochemically and chemically synthesized PPy materials have been compared. From the results of $\sigma_{dc}(T)$, the density of states, and XPS experiments for chemically synthesized PPy−DBSA samples soluble in *m*-cresol solvent, the systems are in an insulating state associated with the reduction of the interchain links or side chains and the weaker interchain interaction. The reduction of the interchain links or side chains of chemically synthesized PPy−DBSA samples compared to electrochemically prepared PPy−PF_6 samples is supported by the relative decrease of the measured area ratio of the disorder effects on the higher energy side through the analysis of C1s decomposed peaks obtained from XPS experiments. The density of states of electrochemically prepared PPy−PF_6 samples is higher than that of soluble PPy. For electrochemically and chemically synthesized PPy systems, we observe the existence of one dopant per three pyrrole rings. The electrochemically synthesized PPy materials have a higher concentration of interchain links or side chains, and are in the critical or the metallic regime. The results agree with expectations of percolation of the metallic state with increasing interchain interaction. The synthesis method using relatively large dopants for soluble PPy materials controls the solubility, the structure, and the charge transport mechanism.

Acknowledgment. This work was supported in part by the CRM-KOSEF (1998) and Korea Science and Engineering Foundation (KOSEF) through Grant 971-0210-043-2. A.J.E. was supported in part by Grant NSF-DMR-95.

References and Notes

(1) Mark, J. A., Ed. *Physical Properties of Polymers Handbook*; American Institute of Physics: New York, 1996; Chapter 34.
(2) Nalwa, H. S., Ed. *Handbook of Organic Conductive Molecules and Polymers*; John Wiley & Sons: New York, 1996; Vols. 1 and 4.
(3) Wang, Z. H.; Li, C.; Epstein, A. J.; Scherr, E. M.; MacDiarmid, A. G. *Phys. Rev. Lett.* **1991**, *66*, 1745.
(4) Conwell, E. M.; Mizes, H. A. *Synth. Met.* **1994**, *65*, 203. Salkola, M. I.; Kivelson, S. A. *Phys. Rev. B* **1994**, *50*, 13962.
(5) Joo, J.; Oblakowski, Z.; Du, G.; Pouget, J. P.; Oh, E. J.; Weisinger, J. M.; Min, Y.; MacDiarmid, A. G.; Epstein, A. J. *Phys. Rev. B* **1994**, *49*, 2977.
(6) Joo, J.; Song, H. G.; Chung, Y. C.; Baeck, J. S.; Jeong, S. K.; Suh, J. S.; Oh, E. J. *J. Korean Phys. Soc.* **1997**, *30*, 230.
(7) Pfluger, P.; Street, G. B. *J. Chem. Phys.* **1984**, *80*, 544.
(8) Kanatzidis, M. G. *Chem., Eng. News* **1990**, *Dec. 3*, 36.
(9) Lee, J. Y.; Kim, D. Y.; Kim, C. Y. *Synth. Met.* **1995**, *74*, 103.
(10) Joo, J.; Lee, J. K.; Hong, J. K.; Baeck, J. S.; Lee, W. P.; Epstein, A. J.; Jang, K. S.; Suh, J. S.; Oh, E. J. *Macromolecules* **1998**, *31*, 479.
(11) Lee, J. K.; Song, H. G.; Joo, J.; Lee, G. J.; Yo, C. H.; Kim, K. H.; Song, S. K.; Jang, K. S.; Oh, E. J. *SaeMulli* (Korean version, ISSN 0374−4914) **1998**, *38*, 16.
(12) Atanasoska, L.; Nao, K.; Smyrl, W. H. *Chem. Mater.* **1992**, *4*, 988.
(13) Tan, K. L.; Tan, B. T. G.; Kang, E. T.; Neoh, K. G. *J. Chem. Phys.* **1991**, *94*, 5382.
(14) Kohlman, R. S.; Joo, J.; Wang, Y. Z.; Pouget, J. P.; Kaneko, H.; Ishiguro, T.; Epstein, A. J. *Phys. Rev. Lett.* **1995**, *74*, 773. Ishiguro, T.; Kaneko, H.; Nogami, Y.; Ishimoto, H.; Nishiyama, H.; Tsukamoto, J.; Takahashi, A.; Yamaura, M.; Hagiwara, T.; Sato, K. *Phys. Rev. Lett.* **1992**, *69*, 660.
(15) Morton, J. R. *Chem. Rev.* **1964**, *64*, 453.
(16) Saunders, B. R.; Fleming, R. J.; Murray, K. S. *Chem. Mater.* **1995**, *7*, 1082.
(17) Mitchell, G. R.; Davis, F. J.; Kiani, M. S. *Br. Polym. J.* **1990**, *23*, 157.
(18) Zabrodskii, A. G.; Zinoveva, K. N. *Sov. Phys. JETP* **1984**, *59*, 425.
(19) Reghu, M.; Yoon, C. O.; Moses, D.; Heeger, A. J.; Cao, Y. *Phys. Rev. B* **1993**, *48*, 17685.

(20) Mott, N. F.; Davis, E. *Electronic Processes in Non-Crystalline Materials*; Clarendon Press: Oxford, England, 1979.
(21) Sato, K.; Yamaura, M.; Hagiwara, T.; Murata, K.; Tokumoto, M. *Synth. Met.* **1991**, *40*, 35.
(22) Prigodin, V. N.; Efetov, K. B. *Phys. Rev. Lett.* **1993**, *70*, 2932.
(23) Samukhin, A. N.; Prigodin, V. N.; Jastrabik, L.; Epstein, A. J. *Phys. Rev. B* **1998**, *58*, 11354.

MA991418O